

# Rutherford Scattering

Kirsten A. Juhl <sup>\*1</sup>, Henriette Ravn <sup>†1</sup>, and Laurits N. Stokholm <sup>‡1</sup>

<sup>1</sup>*Department of Physics and Astronomy, Aarhus University*

September 21, 2018

## Abstract

These experiments studies the Rutherford scattering of protons on atomic nuclei. Energetic 400 keV protons were generated using a Van de Graaff accelerator and directed onto thin metal foils of Au/C, LiF, B, and Al and the scattering cross section of the target atoms was measured as a function of the scattering angle in the range xx to 160 degrees. The cross section showed a clear angular dependency as ..... as expected. The thickness of the target layers Au/C were determined from the stopping power of the layers to be ..... The nuclear reactions of protons with boron were demonstrated by ... Mere is den dur bla bla bla ... In conclusion ...

paper, and to keep our discussion simple and relevant, we will only examine elastic collisions in the semi-classical regime, governed by the Sommerfeld criterion for classical scattering. (Paetz gen Schleck, *Nuclear Reactions: An introduction*, p. 14)

This is usually fine for low energy physics, in which internal energies remain constant and no further particles are created or annihilated. For our experiment, which involves a single Van-de-Graaff accelerator with energies of the order of 400 keV, this will be a very fine approximation.

## 1 Introduction

Almost all of our knowledge in the field of nuclear and atomic physics has been discovered through scattering experiments, and the theory of scattering underpins one of the most ubiquitous tools in physics. Even more, in low energy physics, scattering phenomena provide the standard tool to explore solid state systems. Historically, this was used as a first step towards our current understanding of the atom.

This paper examines the Rutherford scattering of a beam of 400 keV protons with a Au/C solid target. To limit the extend of the

## 2 Materials and Methods

### Experimental Setup

To obtain energies in the order of a 400 keV, a single Van-de-Graaf accelerator (see fig. 1) was used. The variety of incomming beam

---

<sup>\*</sup>201606487@post.au.dk

<sup>†</sup>20116112@post.au.dk

<sup>‡</sup>201605496@post.au.dk



Figure 1: The Van-de-Graaf accelerator.

particles was limited by the source (a flask of hydrogen gas connected to the accelerator tank). Therefore, we only consider incoming ions  $H^+$  and  $H_2^+$ , as the source was stationary, and not changed. Acceleration of the ions was controllable by changing the voltage drop on the dashboard (see fig. 2), and thus also the kinetic energy of the incoming beam. This will be described further in the section Procedure.

The detector was at an angle of the accelerator arm, and by changing the magnetic field strength of the electromagnet, one can choose which of the two possible incoming ions was deflected to interact with the target. The motion of a charged particle in a magnetic field is governed by the Lorentz force law, and as the trajectory of the motion is traced as part of a circle, one obtains the necessary equality for the motion to be<sup>1</sup>

$$F_m = QvB = F_{cp} = \frac{mv^2}{r}. \quad (1)$$

This gives a ratio of the two magnetic fields

---

<sup>1</sup>Dealing with forces and spatial confinements to circular paths is true in the classical regime. Had we wanted a fully relativistic and quantum mechanical description, this would not be the case.



Figure 2: Overview of dashboard. Closer graphics are seen in the Procedure.

needed for the respective ions

$$R_B = \frac{B(H_2^+)}{B(H^+)} = \frac{m(H_2^+)v(H_2^+)}{m(H^+)v(H^+)} \quad (2)$$

$$2 \frac{v(H_2^+)}{v(H^+)} = \sqrt{2} \quad (3)$$

By assuming that the mass of the two ions are related by  $m(H^+) = 2m(H_2^+)$ , and using  $v(X) = \sqrt{\frac{2E}{m(X)}}$  for each ion. Given one of the magnetic fields, the other is determined by this ratio factor. We used the following magnetic fields for the two ions:

$$B(H^+) = 1070 \text{ G} \quad B(H_2^+) = 1513 \text{ G} \quad (4)$$

Conclusively, by changing the magnetic field strength, one changes the incoming ion. BE AWARE: The magnetic field can change over the time scale of measurements due to mechanical heating of the metal in the electromagnet. This leads to expansion and thus the magnetic field will be reduced. From the beamline the particles were directed toward a chosen target material (see fig. 4), where they were scattered on atomic nuclei of the target. A detector was placed at a movable position around the target, such that scattering angles up to 160 degrees could be measured.

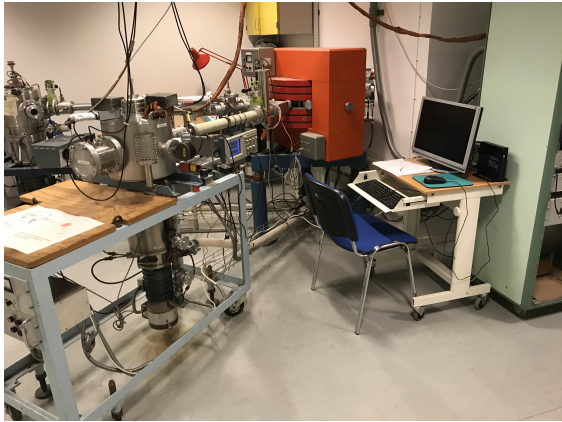


Figure 3: Overview of detector and electromagnet (red brick).

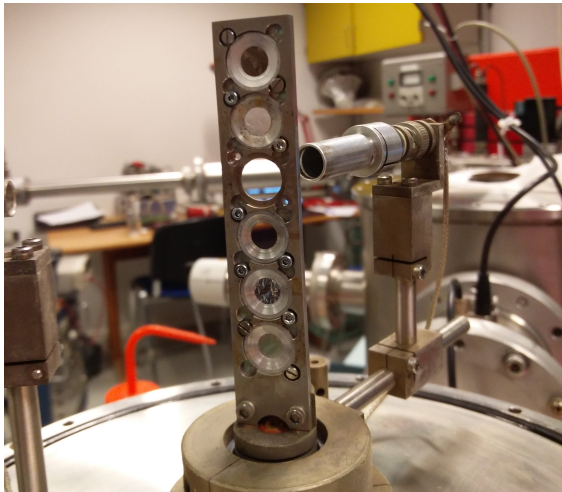


Figure 4: The equipment had a failure, so the targets were changed. We were lucky to get this picture of both detector and targets.

The detector was coupled to a digitizer connected to a computer. During measurements the digitizer started a clock inside it. When the detector was hit by a particle, the digitizer translated the measured energy into a digital number and sent the number and the corresponding time stamp to the computer. The program Mc2Analyzer was used to handle the data. The digital number is an arbitrary number called a channel number. It

is translatable to the actual energy by a linear factor plus an offset. In order to convert these channel numbers to correct energies of the scattered particles a calibration was done.

### Calibration

An energy measurement of the scattered ion gives a digital output, which we call a channel number (or bin number). These hold no physical interpretation, but can be translated to the equivalent energy of the scattered particle. To convert these channel numbers, a calibration is necessary.

Assuming a linear relationship between the energy and the channel number the energy can be found as

$$E = \alpha(k - k_0), \quad (5)$$

where  $k$  is the measured channel and  $k_0$  and  $\alpha$  are parameters. The parameters in the relation is determined by a two step program.

### Determining Zero-Amplitude constant

First, by connecting a pulser (variable output voltage), a relation between the varied energy and the corresponding channel number is obtained. We did this for equidistant pulsed energies, but also the lowest threshold energy. Plotting the count numbers as a function of bin numbers, and fitting a gaussian to each value of pulsed energy, one would obtain all parameters of the gaussian (amplitude, mean value and standard deviation), which was used to estimate the mean bin number, within an uncertainty of the gaussian standard deviation (see fig. 5).

Afterwards, each mean channel number was plotted as a function of the pulser energy, and this surely shows a linear relation, which also was fitted. The intersection is interpreted as the bin number for zero amplitude ( $k_0$ ). A plot can be seen on fig. 6.

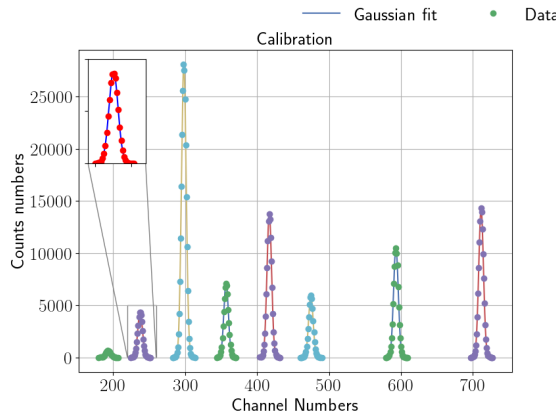


Figure 5: Gaussian fit of all data values. This was used to estimate the mean bin number (channel number), and the uncertainty of this bin number, in the energy-calibration.

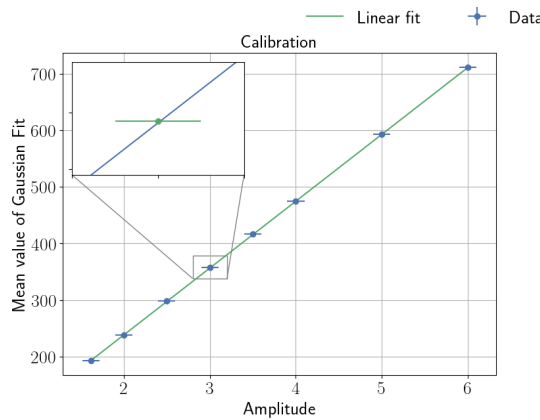


Figure 6: Linear fit of the mean values as a function of amplitude. This was used to determine the zero-amplitude constant  $k_0$ .

## Targets

The targets of interest in this experiment was a thin gold coated carbon plate. The gold coating was about one tenth of the carbon thickness. The thickness of the carbon plate have previously been determined as  $250\text{ \AA}$ , and the thickness of the gold coating as  $25\text{ \AA}$ .<sup>2</sup>

<sup>2</sup>The estimated thickness of each target available have been determined by the previous users of the ex-

The target was placed in holder, which contains several other targets. The height of the holder was fixed, though it was not investigated whether the marked height was optimal in relation to the beam position. When measuring proton scattering at different angles, the blind angles of the target holder may cause a problem. In order to avoid the targets "blind-spots", the target was turned at an angle following the detector while still avoiding the incoming proton beam to end up in a blind angle. The blind angles

## Determining alpha

As described in the previous section, the magnetic field strength of the electromagnet can be adjusted to deflect either  $\text{H}^+$  or  $\text{H}_2^+$  into the beamline. For each of these a data point of energy related to channel number can be found. By considering energy and momentum conservation for elastic scattering in two dimensions the energy of the scattered particles  $E_f$  can be found from the incident proton energy and the scattering angle as:

$$E_f = \left( \frac{m_p \cos \theta + \sqrt{m_t^2 - m_p^2 \sin^2 \theta}}{m_p + m_t} \right)^2 E_i, \quad (6)$$

where  $E_i$  is the energy of the incident beam particles,  $m_p$  and  $m_t$  are the masses of the incident protons and the target particles, respectively, and  $\theta$  is the angle between the direct outgoing non-scattered beam and the scattered particles - also called the scattering angle.

Unfortunately, this only give two data points one from  $\text{H}^+$  and another from  $\text{H}_2^+$ . Nonetheless, the incline from the linear fit to these data points is still useful.

perimental setup and written down on the whiteboard next to the setup.

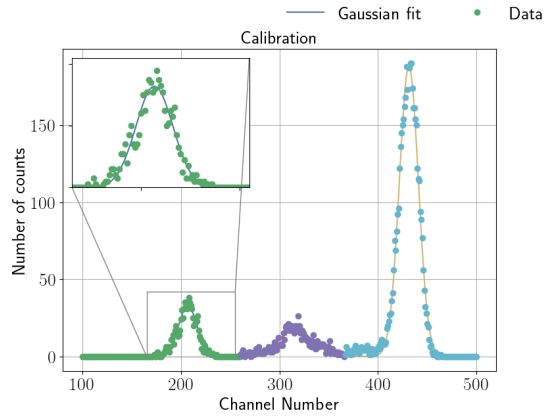


Figure 7: Gaussian fit of all data values. This was used to estimate the mean bin number (channel number), and the uncertainty of this bin number, in the energy-calibration.

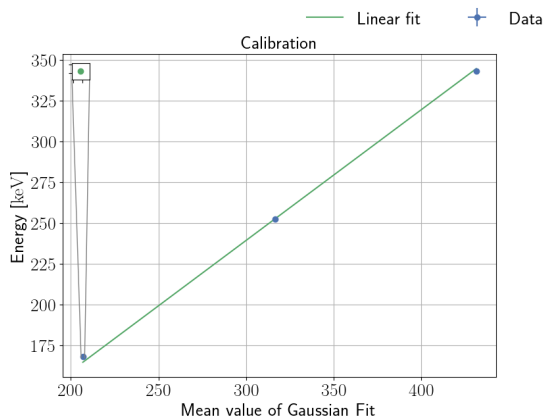


Figure 8: Linear fit of the mean values as a function of amplitude. This was used to determine the zero-amplitude constant  $k_0$ .

## Procedure

First thing, the Van-de-Graaf. To accelerate the beam of incomming particles, one has to generate a hugh potential. Turning on the Belt, one hears the mechanical rhumming. This will generate a potential difference as described further in Krane, *Introduction to Nuclear Physics*, p.xx.



Figure 9: The belt

Now adjust the terminal voltage patiently towards to wanted energy. Our lab instructor advised us to wait for each step, before going to the next.



Figure 10: terminal voltage

Turn on the electromagnet. Remember to calculate the wanted B-field for given element. Look on Faraday cup for received current of particles. Maximize with fine grid (small adjustments).



Figure 11: terminal voltage

When signal is good, set the voltage supply to ...



Figure 12: terminal voltage



Figure 13: process5

## 3 Angular dependency of the Rutherford cross section

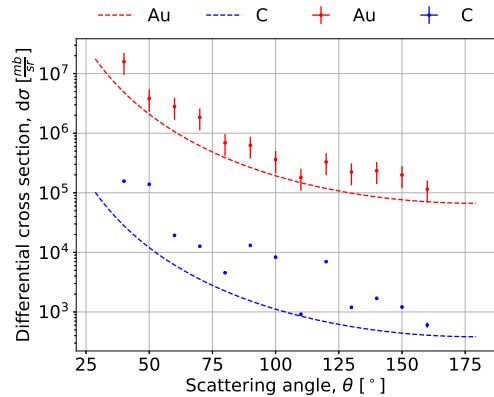


Figure 14: bb

## **4 Angular dependency of the proton energy**

## **5 Target dependency of the Rutherford cross section**

## **6 Thickness of the target layers**

## **7 Nuclear reactions of protons with boron**

## **8 Discussion**

### **The experimental setup**

The Van de Graaf accelerator provide an enormous advantage over the Cockcroft-Walton accelerator as the terminal voltage on a Van de Graaf is extremely stable and does not ripple as the later does. This is very important when desired to measure reaction cross sections. Nonetheless, the Van de Graaf accelerator has a low current output in the  $\mu\text{A}$  range compared with the Cockcroft-Walton  $\text{mA}$ . Nevertheless, this is quite sufficient for nuclear reaction experiments, and thus our chosen accelerator is the workhorse of low-energy nuclear structure physics.

To improve the potential drop across the accelerator:

Vacuum, so the limit of electrical breakdown (sparking) of

To reduce breakdown and sparking, the generator is enclosed in a pressure tank containing an insulating gas. Capacitance (geometrical size)

Krane, *Introduction to Nuclear Physics*

## **9 Conclusion**

## References

Krane, Kenneth S. *Introduction to Nuclear Physics*. 3. John Wiley & Sons, 1987.

Paetz gen Schleck, Hans. *Nuclear Reactions: An introduction*. 3. Springer, 2014. ISBN: 978-3-642-53985-5.